Cost Effective System Using for Bioimpedance Measurement

Nguyen Phan Kien*, Tran Anh Vu
Hanoi University of Science and Technology - No. 1, Dai Co Viet Str., Hai Ba Trung, Ha Noi, Viet Nam
Received: January 22, 2019; Accepted: June 24, 2019

Abstract

This paper presents an economical system for measuring the bioimpedance of meat. The measurement is based on the electrical Fricke model and the inverting configuration of operational amplifiers (op-amp). The system can generate testing signals with frequency ranged from 10Hz to 1MHz and adjustable amplitude up to 1.08Vpp. The sweeping input and output of the op-amp are captured by an oscilloscope that is connected to and controlled by a computer before being processed by MATLAB. The system allows performing automatic customizable sweep routines. Generally, the measurement on a resistor and a RC meat-modeling circuit and a meat sample provided favorable results. In the future, system will be used for measurement and assessment meat quality in order to create a new methods for assessment of food quality.

Keywords: bioimpedance, Fricke model, oscilloscope, MATLAB

1. Introduction

Food quality is now one of the concerning issues in the society. Being popular in many families' daily meals, meat provides a significant amount of nutrient for human body. Thus, the examination of meat freshness is getting more attention of governments and consumers.

To meet these challenged requirements, the evaluation methods need to be exact and fast, using noninvasive technics to estimate the quality. Along with the invasive analysis in the laboratory, the fast checking meat quality methods have been implemented. In [1-4], they use mechanics analysis to evaluate the resistant of the meat [1], [4], to differentiate between raw and well done meat [2], to determine the effects of the measure direction to the probes [3]. Some researches are based on ultrasound measurement, such as ultrasound spectrum analysis [5] and reflection wave measurement [6]. In [7], they differentiate samples by lipid and collagen, which have better results when compared with methods used mechanics and chemistry analysis. [7], [8] shows that the lipid content is correlated with the ultrasound transmission velocity. According to Monin [9], the ultrasound measurement allows users to evaluate the meat structure in live animals well, in an economical and non-invasive way. The optics methods have also been used to test the meat quality such as optics spectrum analysis [10], the infrared spectrum [11], near infrared spectrum [12], Raman spectrum [13], the visible wavelength spectrum [14], color comparison [15] and fluorescent spectrum [16].

Among the methods developed for assessing the meat freshness, bioimpedance analysis is becoming a quick and reasonable approach. The measurement of electrical properties of tissues can reveal the quality of meat based on the impedance parameters of tissues [17]. The dielectric measurement has been considered effective in distinguish the meat age, components and the biochemistry of the meat, which includes biology resistant measurement methods [18], [19], tissue parameterized by microwave [20]. These methodologies can determine whether meat was freeze before or not [19], or involved into the pH measurement of pork or beef, the lipid content and meat age determination.

Systems used in bioimpedance analysis basically consist of dedicated equipment for measuring (i.e. impedance analyzer, LCR meter and dielectric spectroscopy) and a computer for data acquisition and storage [23-25]. Those systems can monitor various bioelectrical parameters of the meat sample with high accuracy and also can perform some advanced functions. However, the spending for such a system on the market is really expensive.

The purpose of this work is to present the design and the operating principle of a cost-effective system used in bioimpedance measurement. In brief, a variable frequency oscillator generates testing signals which are then fed into an inverting op-amp amplifier with the impedance Z of interest on the feedback pathway. The input and output signals of the amplifier are recorded. The acquisition, storage and processing of the data are controlled by MATLAB, in which there are two parameters of interest: magnitude and phase of Z. Evaluation of the reliability of the

* Corresponding author: Tel.: (+84) 944.639.471
Email: kien.nguyenphan@hust.edu.vn

system as a tool to investigate bioimpedance is also provided in this work.

The paper is organized as follows. Section II describes the methodologies and materials used for the research. Section III presents the experiments and the results. Section IV concludes the paper.

2. Methodologies and materials

2.1. Meat modeling

To investigate impedance of biological tissue, it is necessary to view it according to an electrical model. One of the first successful electrical model was proposed by Fricke [21], [22], which has been used extensively in research into cells or micro-organisms in suspension in a liquid medium [23]. Fricke considered biological tissue as ionized liquid medium (i.e. extracellular fluid (ECF)) suspending cells, which was intracellular fluid (ICF) enclosed by insulating membranes. Also, components of biological tissue (cell membranes, ICF, ECF) were represented by passive electrical elements [23]. The equivalent circuit represented tissue is shown in Fig.1. R_e, R_i, C_m respectively are resistance of ECF, ICF and capacitance of membrane.

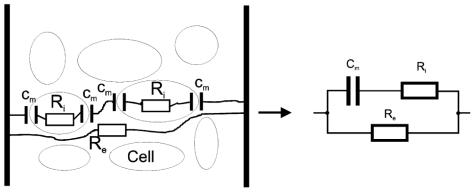

Fig. 1. Equivalent circuit of Fricke model

Because of properties of the capacitance, at low frequency, current tends to flow in ECF outside the cells. The higher the frequency, the more alternating current passes through the cell membranes, hence ICF. According to Fricke model, equivalent complex impedance of biological tissue can be described in equation (1).

$$Z = R_e \,/\!/ \left(R_i + \frac{1}{j\omega C_m}\right)$$

$$= Re(Z) + jIm(Z) = |Z|e^{j\theta} \qquad (1)$$

In which

$$\omega = 2\pi f; \qquad |Z| = \sqrt{\left(Re(Z)\right)^2 + \left(Im(Z)\right)^2};$$

$$\theta = Arg(Z) = arctan\left(\frac{Im(Z)}{Re(Z)}\right)$$

where *Re(Z), Im(Z)* are the real and imaginary parts respectively, $|Z|$ is magnitude of Z, θ is phase or argument of Z, f is the frequency of current applied to the tissue. Changes in structural properties of tissue will reflect on R_e, R_i, C_m, hence $|Z|$ and θ.

2.2. System design

2.2.1. General operation

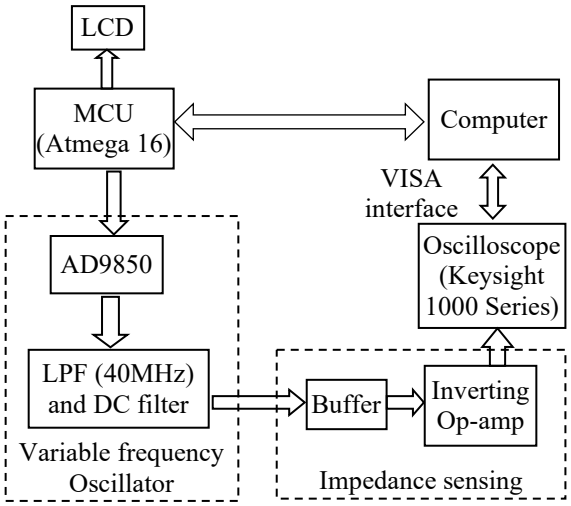

Fig. 2. Block diagram of the system

Hardware structure of the system is presented by the diagram in Fig. 2. The system consists of five blocks namely Microprocessor, Oscilloscope, Computer, Variable frequency oscillator (VFO), and Impedance sensing. Roles of the Microprocessor is to control VFO. It stores a list of sweeping frequencies to feed into the VFO to generate different programmed frequencies. As for the computer, it will communicate with the Oscilloscope through a VISA interface to control and acquire data from it after receiving a certain message from the Microprocessor. Another task of the Computer is to save data and conduct further analysis to obtain $|Z|$ and θ of an investigated biological tissue.

The VFO block contains 3 main parts: AD9850, a 40MHz low-pass filter and a DC filter (1Hz high-pass filter). VFO contains a 40-bit register that is used to program the 32-bit frequency control word, the 5-bit phase modulation word, and the power-down function. The code can be loaded into the register via a serial method. The 32-bit tuning word is used to program desirable output frequency according to the formula

$$f_{OUT} = (Tuning\ word \times CLKIN)/2^N \qquad (2)$$

where CLKIN is the input reference clock frequency in MHz, f_{OUT} is the frequency of the output signal in MHz, N is the number of bits in the tuning word, and equals 32. Incremental resolution of frequency is determined by the formula

$$Resolution = CLKIN/2^N \qquad (3)$$

In this project a 125MHz clock-source was used as the clock reference for AD9850, then the

resolution can reach to 0.0291 Hz. In addition, the AD9850's circuit architecture allows the generation of output frequencies of up to one-half the reference clock frequency (or 62.5 MHz).

In fact, actual signal obtained is always contaminated by high-frequency noise. A low-pass filter is therefore needed to make the signal cleaner. A high-order 40MHz elliptic filter is recommended. R_1 and R_2 were selected with similar values for the purpose of matching the input and output impedances of the filter.

2.2.2. *Impedance sensing block*

Fig. 3 shows the Impedance sensing block. This block consists of two op-amps LMP8671, one for buffer and the other for amplification. LMP8671 is the high precision, low noise amplifier with Gain Bandwidth Product up to 55MHz. This bandwidth is quite suitable for the desirable sweeping range of the system (10Hz-1MHz). From the inverting configuration of the Op-amp, the relation between impedance Z and resister RG is presented in equation (4):

$$-\frac{Z}{R_G} = \frac{V_{out}}{V_{in}} \tag{4}$$

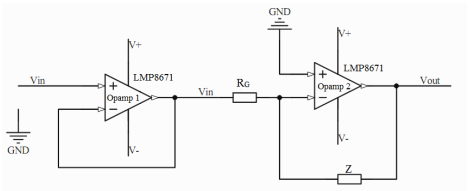

Fig. 3. Schematic drawing of the Impedance sensing block

2.2.3. *Oscilloscope control from MATLAB*

The 2-channel oscilloscope utilized in this system is DSO1012A (1000 Series Portable Oscilloscopes from Agilent Technologies) with bandwidth from DC to 100MHz. This instrument also features a maximum sample rate of 2 GSa/s, a maximum memory depth of 20 kpts. If two channels are both turned on, the Fig.2 for each channel are 1 GSa/s, and 10 kpts.

The most significant feature of this device is that it is a digital oscilloscope, thus it can be controlled directly from MATLAB using Instrument Control Toolbox.

2.2.4. *Generate magnitude and phase of impedance*

Suppose input and output signals from Op-amp 2 (Fig.3) have center frequency f, then:

$$V_{out} = A_{out}\sin(2\pi ft + \varphi_{out}) = A_{out}e^{j\varphi_{out}}$$
$$V_{in} = A_{in}\sin(2\pi ft + \varphi_{in}) = A_{in}e^{j\varphi_{in}} \tag{5}$$

A_{in}, A_{out} are amplitude of the component with frequency f of the input and output signals. φ_{in}, φ_{out} are respectively their phases.

$$(4) \Rightarrow \frac{Z}{R_G} = \frac{A_{out}e^{j\varphi_{out}}}{A_{in}e^{j\varphi_{in}}} \tag{6}$$

$$\left|\frac{Z}{R_G}\right| = \left|-\frac{A_{out}e^{j\varphi_{out}}}{A_{in}e^{j\varphi_{in}}}\right| \Rightarrow |Z| = R_G\frac{A_{out}}{A_{in}} \tag{7}$$

$$Arg\left(\frac{Z}{R_G}\right) = Arg\left(-\frac{A_{out}e^{j\varphi_{out}}}{A_{in}e^{j\varphi_{in}}}\right)$$

$$\Rightarrow Arg(Z) - Arg(R_G) = Arg(-A_{out}e^{j\varphi_{out}}) - Arg(A_{in}e^{j\varphi_{in}}) \tag{8}$$

$$\Rightarrow \theta = \pi + \varphi_{out} - \varphi_{in} \tag{9}$$

(φ_{out} - φ_{in}) is essentially the phase shift between output and input signals.

This idea was implemented in MATLAB with the help of Fast Fourier Transform (FFT) function. FFT was applied on both V_{in} and V_{out} to convert them from time domain into frequency domain. Each result was then searched for the frequency component with peak magnitude. Eventually, A_{in}, A_{out}, φ_{in}, φ_{out} were obtained. Based on Equation (7) and (9), $|Z|$ and θ can be computed.

3. Experimental results and discussion

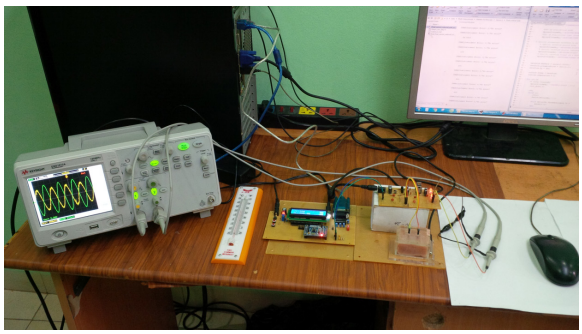

Fig. 4. The entire system

The whole system is presented in Fig. 4

All experiments in this research entailed frequency sweep. The sweeping range was from 10Hz to 1MHz, containing 46 frequency. In addition, R_4 was set to zero in all tests. It should also be noted that because the main focus was bioimpedance.

3.1. Test output of the VFO

One channel of the Oscilloscope is connected to the output of impedance sensing circuit (Fig.3) and data is then saved in the Computer at each sweeping frequency. Each data was converted from time domain into frequency domain using FFT command in MATLAB to find the component with maximum amplitude, i.e. the center frequency. The obtained amplitude and center frequency were then compared

with theoretical ones. Since R_4 = 0, according to equation (6), V_{pp} (at node C) was expected to be around 1.024V at all frequencies. In addition, amplitude spectrum of an output sine wave was expected to have a single peak at the frequency close to the corresponding value input to the VFO.

Actual frequency	Theoretical frequency	Actual frequency	Theoretical frequency
10.070	10	6000.06	6000
20.000	20	7000.07	7000
30.000	30	8000.08	8000
40.000	40	9000.09	9000
50.001	50	10000.1	10000
60.001	60	20000.2	20000
70.001	70	30000.3	30000
80.001	80	40000.4	40000
90.001	90	50000.5	50000
100.001	100	60000.6	60000
200.002	200	70000.7	70000
300.003	300	80000.8	80000
400.004	400	90000.9	90000
500.005	500	100001.0	100000
600.006	600	200002.0	200000
700.007	700	300003.0	300000
800.008	800	400004.0	400000
900.009	900	500005.0	500000
1000.01	1000	600006.0	600000
2000.02	2000	700007.0	700000
3000.03	3000	800008.0	800000
4000.04	4000	900009.0	900000
5000.05	5000	1000010.0	1000000

Table 1. Sweeping frequencies from 10Hz to 1MHz

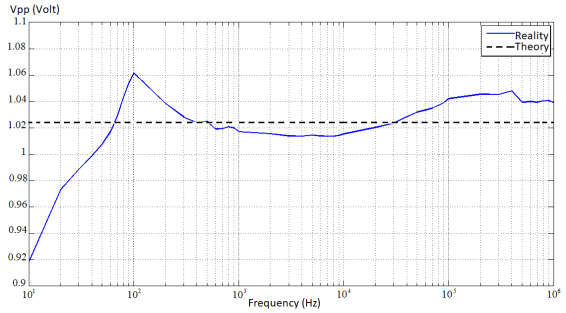

Fig. 5. Actual and theoretical estimation of Vpp of center frequencies

Desirable frequencies and the actual center frequencies are compared in Table 1. Compared to desirable frequency, while error at 10Hz equals 0.701%, the data for other frequencies were all around 0.001%.

Actual and theoretical estimation of V_{pp} of center frequencies are presented in Fig. 5. Compared to the theory, while error at 10Hz equals 10.25%, the Fig.s for other frequencies were all less than 5%. RMSE equals 0.0227V.

3.2. Test with Z as a resistor

Test was conducted with R_G = 220.3Ω, and Z = 467.7 Ω. These values were obtained by measuring the chosen resistors with a multimeter. V_{in} and V_{out} of Op-amp 2 (Fig.3) were recorded and saved in the Computer at each sweeping frequency. Data analysis was then carried out to obtain $|Z|$ and θ. For each case, $|Z|$ was expected to be close to the actual value and θ was expected to be close to zero at all frequencies.

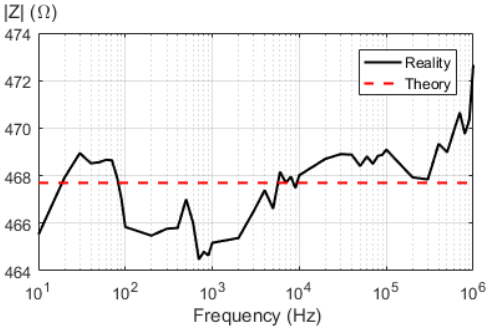

Fig. 6. Actual and theoretical estimation of $|Z|$

Actual and theoretical estimation of $|Z|$ throughout sweeping frequencies are presented in Fig.6. Compared to the theory, maximum error equals 1.06% and RMSE equals 1.725Ω.

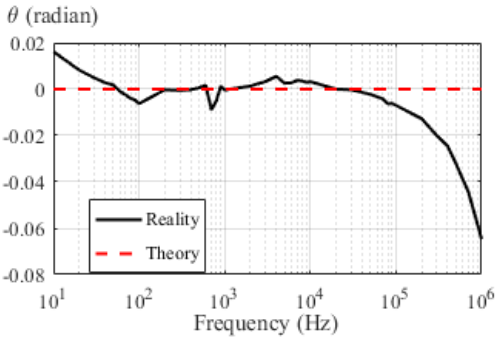

Fig. 7. Actual and theoretical estimation of θ

Actual and theoretical estimation of θ throughout sweeping frequencies are presented in Fig.7. Compared to the theory, maximum error equals 0.065 radian and RMSE equals 0.019 radian.

3.3. Test with Z as a meat-modeling circuit

A RC-circuit was used mimic electrical behavior of a biological tissue (Fig.1). In this test, R_G=464.0Ω, R_i=171.1Ω, R_e=2161.0Ω, C_m=7.0nF. These values were obtained by measuring the chosen resistors with a multimeter. The same procedure as in previous part is implemented. Since $|Z|$ would change

with frequency, value of R_G was chosen to be between R_{10} and R_{1M}, which were $|Z|$ at 10Hz and 1MHz respectively. R_{10} and R_{1M} were estimated visually using the Oscilloscope prior to conducting an automatic sweep. $|Z|$ and θ was expected to be close to the theoretical calculation at all frequencies.

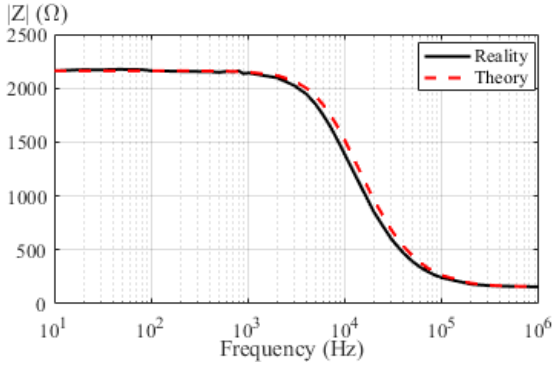

Fig. 8. Actual and theoretical estimation of $|Z|$

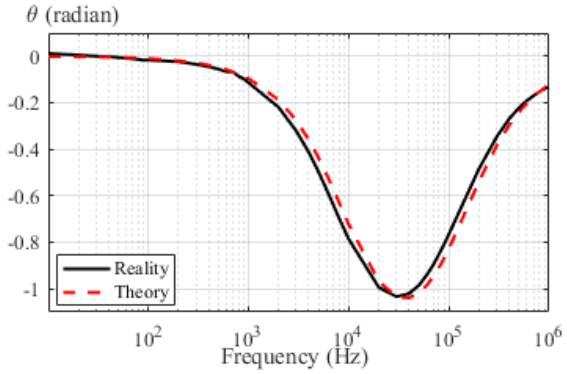

Fig. 9. Actual and theoretical estimation of θ

Actual and theoretical estimation of $|Z|$ throughout sweeping frequencies are presented in Fig.8. Compared to the theory, maximum error equals 12.18% and RMSE equals 49.630Ω.

Actual and theoretical estimation of θ throughout sweeping frequencies are presented in Fig.9. Compared to the theory, maximum error equals 0.068 radian and RMSE equals 0.035 radian.

3.4. Test with Z as a piece of pork

Main purpose of this test is to observe bioimpedance of a piece of pork in 10 routines, with a period of 57 minutes between 2 consecutive ones. Sweeping range was between 100Hz to 1MHz. Stainless steel rod-shaped electrodes and case are shown in Fig.10. A case was used to minimize influence of humidity and to fix electrodes' position. The same procedure as in previous part is implemented.

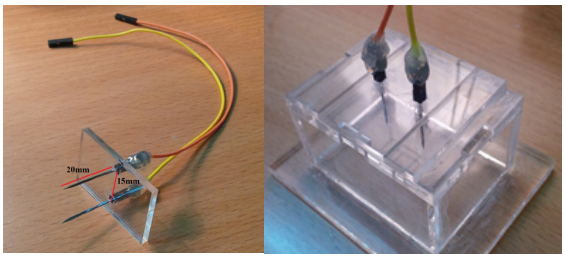

Fig. 10. Stainless steel electrodes (left) and electrodes joining on the top of the case (right)

$|Z|$ and θ throughout sweeping frequencies are presented in Fig.11 and Fig.12. From these graphs, impedance of the meat sample behaved in a relatively similar manner as the RC model above in terms of both $|Z|$ and θ

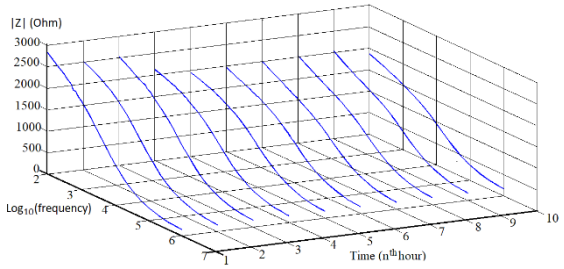

Fig. 11. $|Z|$ throughout 10 routines of measurement

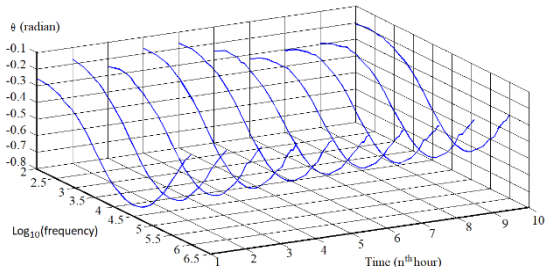

Fig. 12. θ throughout 10 routines of measurement

4. Conclusion

This paper presents a cost-effective system for measuring bioelectrical impedance. The measuring principle is based on electrical Fricke model and the op-amp's inverting amplifier configuration. The experimental tests on a resistor and a RC meat-modeling circuit and a meat sample reveal some promising results. The system can be improved in the future when investigating bioimpedance of meat samples.

Acknowledgments

This research is funded by the Hanoi University of Science and Technology (HUST) under project number T2017-PC-118.

References

[1]. J. Lepetit, J. Culioli;Mechanical-properties of meat; Meat Science, vol. 36 (1-2), pp.203-237, 1994.

[2]. E. Tornberg; Biophysical aspects of meat tenderness". Meat Science, vol. 43, S175-S191, 1996.

[3]. J. W. Stephens, J. A. Unruh, M. E. Dikeman, M. C. Hunt, T. E. Lawrence, and T. M. Loughin; Mechanical probes can predict tenderness of cooked beef longissimus using uncooked measurements; Journal of Animal Science, vol. 82 (7), pp.2077-2086, 2004.

[4]. S. D. Shackelford, T. L. Wheeler, and M. Koohmaraie "Evaluation of slice shear force as an objective method of assessing beef longissimus tenderness; Journal of Animal Science, vol. 77 (10), pp. 2693-2699, 1999.

[5]. S. Abouekaram, P. Berge, and J. Culioli; Application of ultrasonic data to classify bovine muscles; Proceedings of IEEE Ultrasonics Symposium, vol. 2, pp. 1197-1200, 1997.

[6]. J. Ophir, R. K. Miller, H. Ponnekanti, I. Cespedes, and A. D. Whittaker; Elastography of beef muscle; Meat Science, vol. 36 (1-2), pp. 239-250, 1994.

[7]. S. Abouelkaram, K. Suchorski, B. Buquet, P. Berge, J. Culioli, P. Delachartre, and O. Basset. "Effects of muscle texture on ultrasonic measurements; Food Chemistry, vol. 69, pp. 447-455, 2000.

[8]. J. Benedito, J. A. Carcel, C. Rossello, and A. Mulet; Composition assessment of raw meat mixtures using ultrasonics;Meat Science, vol. 57 (4), pp. 365-370, 2001.

[9]. G. Monin; Recent methods for predicting quality of whole meat; Meat Science, vol. 49 (1), S231-S243, 1998.

[10]. K. I. Hildrum, J. P. Wold, H. S. Vegard, J.P. Renou, and E. Dufour; New spectroscopic techniques for on-line monitoring of meat quality; Advanced technologies for meat processing, CRC Press. pp. 87-129, 2006.

[11]. T. Kempen; Infrared technology in animal production; Worlds Poultry Science Journal, vol. 57 (1), pp. 29-48, 2001.

[12]. S. D. Shackelford, T. L. Wheeler, and M. Koohmaraie; On-line classification of US Select beef carcasses for longissimus tenderness using visible and nearinfrared reflectance spectroscopy; Meat Science, vol. 69 (3), pp. 409-415, 2005.

[13]. A. M. Herrero; Raman spectroscopy a promising technique for quality assessment of meat and fish: A review; Food Chemistry, vol. 107 (4), pp. 1642-1651, 2008.

[14]. J. Xia, A. Weaver, D. E. Gerrard, and G. Yao; Monitoring Sarcomere Structure Changes in Whole Muscle Using Diffuse Light Reflectance; Journal of Biomedical Optics, vol. 11 (4), 2006.

[15]. J. Xing, M. Ngadi, A. Gunenc, S. Prasher, and C. Gariepy; Use of visible spectroscopy for quality classification of intact pork meat; Journal of Food Engineering, vol. 82 (2), pp. 135-141, 2007.

[16]. G. Yao, K. S. Liu, and F. Hsieh; A new method for characterizing fiber formation in meat analogs during high-moisture extrusion; Journal of Food Science, vol. 9 (7), pp. E303-E307, 2004.

[17]. C.E. Byrne, D.J. Troya, and D.J. Buckley; Postmortem changes in muscle electrical properties of bovine M. longissimus dorsi and their relationship to meat quality attributes and pH fall; Meat Science, vol. 54, pp. 23-34, 2001.

[18]. J. Lepetit, J. L. Damez, S. Clerjon, R. Favier, S. Abouelkaram, and B. Dominguez; Multielectrode sensor for measurement of electrical anisotropy of a biological material [e.g. meat] and utilization of the sensor; French Patent Application (FR2880124-B1), 2007.

[19]. J. L. Damez, S. Clerjon, S. Abouelkaram, and J. Lepetit; Beef meat electrical impedance spectroscopy and anisotropy sensing for non-invasive early assessment of meat ageing; Journal of Food Engineering, vol. 85 (1), pp. 116-122, 2008.

[20]. S. Clerjon, J. D. Daudin, and J. L. Damez; Water activity and dielectric properties of gels in the frequency range 200MHz-6 GHz; Food Chemistry, vol. 82, pp. 87-97, 2003.

[21]. H. Fricke; A Mathematical Treatment of the Electric Conductivity; Physical Review, vol. 24, no. 5, pp. 575-587, 1924.

[22]. H. Fricke; A mathematical treatment of the electric conductivity and; Physical Review, vol. 26, no. 5, pp. 678-681, 1925.

[23]. J.L. Damez, S. Clerjon, S. Abouelkaram, and J. Lepetit; Dielectric behavior of beef meat in the 1-1500 kHz range: Simulation with the Fricke/Cole-Cole model; Meat Science, vol. 77, pp. 512-519, 2007.

[24]. K. N. Khamil and C. K. Yin; An Analysis of Lard by using Dielectric Sensing Method; Journal of Telecommunication, Electronic and Computer Engineering, vol. 8, pp. 131-137, 2016.

[25]. D.T. Trung, N.P. Kien, T.D. Hung, D.C. Hieu and T.A Vu; Electrical impedance measurement for assessment of the Pork aging: a Preliminary study; Third International Conference of Biomedical Engineering, pp. 95-99, 2016.